Residual stress analysis with stress-dependent growth rate and creep deformation during oxidation

Yaohong Suo[a),b)]
School of Mechanical Engineering and Automation, Fuzhou University, Fuzhou 350108, China; and School of Science, Xi'an University of Science and Technology, Xi'an 710054, China

Zhonghua Zhang[b)]
School of Science, Xi'an University of Science and Technology, Xi'an 710054, China

Xiaoxiang Yang[b)]
School of Mechanical Engineering and Automation, Fuzhou University, Fuzhou 350108, China

(Received 8 March 2016; accepted 27 June 2016)

In this paper, taking into account the external loading, growth strain, creep, and bending deformation during the metallic high-temperature oxidation, a residual stress evolution model is developed according to the force- and moment-equilibrium equations. In this model, oxidation kinetic relationship (the stress-dependent growth rate) is related to the stress in the oxide scale, not classical parabolic law. If and only if the stress in the scale or the activation volume is equal to zero, this relationship can reduce to the parabolic law. Then the stress-dependent oxidation kinetics is compared with the stress-independent one (the parabolic law). Finally, effects of the external loading on the stress distribution in the oxide scale, the curvature of the system and the scale thickness are discussed, and numerical results show that the tensile external loading decreases the oxidation stress and promotes the growth rate of the oxidation layer.

I. INTRODUCTION

When metals or alloys are subjected to an aggressive oxidizing environment at high temperature, the residual stress is inevitably generated.[1–3] Furthermore, the stress distribution can influence the oxidation kinetics (i.e., growth of the scale). It is greatly important to determine the stress field together with the growth of the oxide film, and this is because the lifetime of high-temperature metals or alloys is controlled by the stress and the oxidation resistance. Generally speaking, the oxidation resistance depends on the mechanical properties of the forming oxidation scale whether it can prevent the underlying metal substrate from further oxidation. Evans[4] pointed out that Alumima was often regarded as a barrier for oxygen diffusion because its oxide Al_2O_3 had excellent properties at high temperature, superior adherence, and slow growth rate compared with other oxides.[5,6] The mechanism of the stress generation is not completely clear. Therefore, the stress analysis during oxidation has attracted more and more attention.

At present, the main possible origins of the stress generation include: (i) epitaxy relationships between metal substrate and oxide scale (lack of compatibility of the crystalline lattices).[7,8] The epitaxy is an interface phenomenon and the growth of a thin layer on a substrate generally coincides with an incompatibility of the two crystalline lattices (i.e., lattice mismatch). Generally, the lattice parameter of an oxide is significantly larger than that of the metal. This large lattice mismatch[9–11] makes the formation of coherent metal–oxide interface energetically unfavorable. Thus a mismatch strain necessarily accommodates the difference in the lattice parameters at the interface and decreases away from the boundary where the lattice is relaxed. This phenomenon induces stresses at a microscopic level. (ii) Mismatch in the coefficients of thermal expansion and molar volume between the film and the substrate.[12–14] (iii) Phase transformation,[15,16] densification, spallation, failure,[4,17] and even crack.[18] These show that the oxidation can lead to the generation of the stresses. (iv) The possibility that the oxide grows in the oxide grain boundaries. (v) The oxygen dissolution in the metal or alloy.[16]

Taking aim at these origins, various models have been developed to describe the stress evolution during oxidation. Evans[4] and Limarga et al.[19,20] developed stress and diffusion behavior model. Zhou et al.,[21] Wang et al.,[22] and Suo et al.[23] took into account the interplays among the chemical reaction, diffusion and stress and developed the corresponding coupled models. Panicaud et al.[24] proposed a new explanation for the proportional dependence between the growth strain and the thickness of the oxide scale, and developed the viscoplastic stress evolution model. Maharjan et al.[10,25] gave some analysis

Contributing Editor: Susan B. Sinnott
[a)]Address all correspondence to this author.
e-mail: yaohongsuo@126.com
[b)]These authors contributed equally to this manuscript.
DOI: 10.1557/jmr.2016.262

models to predict growth stress and strain during symmetric oxidation based on the force balance equation and the strain compatibility at the oxide/metal interface. Ruan et al.[26,27] considered the bending deformation and presented theoretical stress analysis model with growth strain and creep strain based on the force and moment balance equation. However, the oxidation growth (i.e., the thickness of the scale) is simply regarded to abide by the parabolic law in these above models. Additionally, growth strain satisfies the Clarke's assumption (i.e., the growth strain rate is proportional to the rate of the thickness). Hu and Shen[28] adopt the variational principle method to develop a thermal–chemical–mechanical fully coupling model. In their theory, the growth strain is affected by the stress, the affinity of the reaction and so on in the evolving equations (the second constitutive equation) rather than simple Clarke's assumption. Suo et al.[29,30] developed the stress evolution model with the chemo-mechanical coupled effect in the growth strain relationship on basis of Hu and Shen's theory. These models mentioned above can describe and predict the stress evolution to some extent while the growth rate is too simple (the parabolic law). Zhang et al.[31] and Dong et al.[32] derived the residual stress analysis under the stress-dependent oxidation kinetics relationship. The discrepancy of them is that Zhang et al.'s model[31] added the creep effect on the basis of Dong et al.'s model.[32] However the bending deformation during oxidation was not taken into account in their models. In addition, it is not appropriate that H is a constant in the theoretical research[32] because the sum of h_{ox} (thickness of the scale) and h_s (thickness of the substrate) is variable during oxidation and does not always equal H (constant).

Based on these above points, the purpose of this paper is to consider the bending deformation, stress-dependent oxidation kinetic relationship instead of simple parabolic law, growth strain and creep effect, the evolution equations of the stress and curvature are developed in terms of the force and moment-equilibrium equations. For FeCrAlY isothermal oxidation, we discuss the influence of the external loading on the stress in the oxide, the curvature of the system and the scale thickness.

II. STRESS-DEPENDENT GROWTH RATE MODEL FOR THE STRESS EVOLUTION

Metal oxidation at high temperature is schematically shown in Fig. 1. The external loading $\sigma_{external}$ is applied to the system. The thicknesses of the oxidation scale and the metal substrate are h_{ox} and h_s, respectively. The origin of the system is set at the central of the substrate. Suppose that (i) the mechanical properties of the oxide scale and substrate are isotropic. (ii) Isothermal oxidation occurs on single surface of the metal. (iii) The other surface is protected by the oxide coating as described by Saunders et al.[34]

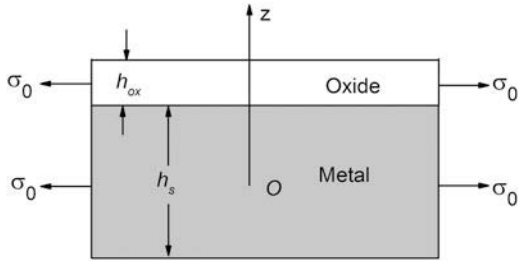

FIG. 1. A schematic of metal oxidation.

For some metals or alloys, the oxidation at high temperature is controlled by the diffusion rate of the oxygen anions and metal cations in the formed oxide scale due to the fast reaction at the gas/oxide surface or oxide/substrate interface. The oxidation kinetics (i.e., the thickness rate of the scale) relationship dependent of the oxidation stress is presented as[31]

$$\frac{\mathrm{d}h_{\mathrm{ox}}}{\mathrm{d}t} = D\frac{c_1 - c_2}{h_{\mathrm{ox}}} \quad , \tag{1}$$

where t is the oxidation time, D is the diffusion coefficient, c_1 and c_2 represent the vacancy concentration at the gas/oxide surface and oxide/substrate interface in the case of no stress. During the process of oxidation, diffusion coefficient D influenced by the stress in the oxide can be expressed as[35,36]

$$D = D_0 \exp\left(\frac{\sigma_{\mathrm{ox}}\Delta\Omega}{RT}\right) \quad , \tag{2}$$

where D_0 is the diffusion coefficient independent of stress. R, T, and σ_{ox} are the Boltzmann's constant, the absolute temperature and the stress in the oxide, respectively. The activation volume $\Delta\Omega$, which is associated to the Pilling–Bedworth ratio (PBR), can be expressed as[4]

$$\Delta\Omega = (\mathrm{PBR} - 1)\cdot\Omega_{\mathrm{m}} \quad ,$$

where Ω_m is the volume of the metal per metal ion.

Combining Eqs. (1) and (2), one obtains

$$h_{\mathrm{ox}}(t) = k_{\mathrm{p}}\left[\int_0^t \exp\left(\frac{\sigma_{\mathrm{ox}}\Delta\Omega}{RT}\right)\mathrm{d}t\right]^{1/2} \tag{3}$$

where $k_p = \sqrt{2D_0(c_1 - c_2)}$ is the oxidation kinetics constant. It is worth noticing that Eq. (3) can be simplified into the conventional parabolic form if the value of $\Delta\Omega$ or σ_{ox} is zero.

When the metal is exposed to the high-temperature oxidation atmosphere, the oxide scale generally grows laterally as well as thickening without the constraint of the metal substrate during the process of isothermal

oxidation, as shown in Fig. 1. Meanwhile the growth strain is accompanied to occur. According to the microstructure approach proposed by Clarke,[11] the lateral growth strain rate, $\dot{\varepsilon}_g(t)$, of the oxide scale is given as

$$\dot{\varepsilon}_g(t) = D_{ox}\dot{h}_{ox}(t) \quad , \tag{4}$$

where ε_g represents the growth strain, and D_{ox} is the lateral growth constant. The superposed dot denotes differentiation with respect to the time.

The oxide film is adherent to the metal surface so that the oxide scale can not freely expand in the lateral direction. The substrate constraint products elastic strain and the corresponding elastic strain in the oxide scale. In addition, creep deformations will be caused to occur in both oxide and substrate. In this section, neglecting the creep deformation and taking into account the elastic strain in both the oxide and metal, and the growth strain in the oxide, in conjunction with thermal expansion strain, the total strain in the system during high-temperature oxidation is expressed as

$$\begin{aligned} \varepsilon_{ox}(t) &= \varepsilon^e_{ox}(t) + \alpha_{ox}\Delta T + \varepsilon_g(t) \quad h_s/2 < z < h_s/2 + h_{ox} \\ \varepsilon_s(z,t) &= \varepsilon^e_s(z,t) + \alpha_s\Delta T \qquad -h_s/2 < z < h_s/2 \quad , \end{aligned} \tag{5}$$

where ε, ε^e, ΔT, and α are the total strain, elastic strain, the temperature change, and the thermal expansion coefficient, respectively.

Due to the single surface oxidation, the system will bend and the curvature can be observed. According to the plane assumption, the total strain can be given as

$$\begin{aligned} \varepsilon_{ox}(t) &= \varepsilon_0(t) - k(t)\frac{h_s}{2} \qquad h_s/2 < z < h_s/2 + h_{ox} \\ \varepsilon_s(z,t) &= \varepsilon_0(t) - k(t)z \qquad -h_s/2 < z < h_s/2 \quad , \end{aligned} \tag{6}$$

where $\varepsilon_0(t)$ is the lateral strain at the interface of the scale/metal system, and $k(t)$ is the curvature of the deformed neutral axis.

In terms of the generalized Hooke's law for the equivalent biaxial stress and combining Eq. (5) with (6), the stresses in the system can be written as

$$\begin{aligned} \sigma_{ox}(t) &= M_{ox}\left[\varepsilon_0(t) - k(t)\frac{h_s}{2} - \alpha_{ox}\Delta T - \varepsilon_g(t)\right] \quad h_s/2 < z < h_s/2 + h_{ox} \\ \sigma_s(z,t) &= M_s[\varepsilon_0(t) - k(t)z - \alpha_s\Delta T] \quad -h_s/2 < z < h_s/2 \quad , \end{aligned} \tag{7}$$

where σ is the equi-biaxial stress of the system; $M_{ox} = \frac{E_{ox}}{1-\nu_{ox}}$, $M_s = \frac{E_s}{1-\nu_s}$ are the biaxial modulus; E and ν are the Young's modulus and Poisson's ratio, respectively.

To keep balance during oxidation, the following equilibrium equations of forces and moments must be satisfied:

$$\begin{aligned} \int_{-h_s/2}^{h_s/2}\sigma_s dz + \sigma_{ox}h_{ox} &= \sigma_{external}(h_{ox} + h_s) \\ \int_{-h_s/2}^{h_s/2}\sigma_s z dz + \sigma_{ox}h_{ox}\left(\frac{h_s}{2} + \frac{h_{ox}}{2}\right) &= \sigma_{external}h_{ox}\left(\frac{h_{ox}}{2} + \frac{h_s}{2}\right) \quad . \end{aligned} \tag{8}$$

Combining Eqs. (4), (7) and (8), the lateral strain of the central plane in the substrate, ε_0, and the curvature of the system are solved as follows:

$$\varepsilon_0(t) = A_1\varepsilon_g(t) + A_1\alpha_{ox}\Delta T + A_2\alpha_s\Delta T + A_3\sigma_{external} \tag{9a}$$

$$k(t) = -\frac{6(h_s + h_{ox})}{h_s^2}\left[A_1\varepsilon_g(t) - A_1\alpha_s\Delta T + A_1\alpha_{ox}\Delta T\right] + A_4\sigma_{external} \tag{9b}$$

with

$$\begin{aligned} A_1 &= \frac{h_s M_{ox} h_{ox}}{h_s^2 M_s + 4M_{ox}h_{ox}h_s + 3M_{ox}h_{ox}^2} \\ A_2 &= \frac{h_s^2 M_s + 3h_s M_{ox}h_{ox} + 3M_{ox}h_{ox}^2}{h_s^2 M_s + 4M_{ox}h_{ox}h_s + 3M_{ox}h_{ox}^2} = 1 - A_1 \\ A_3 &= \frac{h_s + h_{ox}}{M_s}\cdot\frac{M_s h_s + 3M_{ox}h_{ox}}{h_s^2 M_s + 4M_{ox}h_{ox}h_s + 3M_{ox}h_{ox}^2} \\ A_4 &= \frac{6h_{ox}(h_s + h_{ox})}{M_s h_s}\cdot\frac{M_{ox} - M_s}{h_s^2 M_s + 4M_{ox}h_{ox}h_s + 3M_{ox}h_{ox}^2} \quad . \end{aligned} \tag{10}$$

It is noted that the initial creep strain in both oxide and metal substrate are zero when $t = 0$. Thus, Eq. (9) can be applied to the initial condition of the following creep model for the stress evolution. This is why the creep strain is neglected in this part. It is not only an elastic model but also the initial condition of the creep model.

III. THE CREEP MODEL FOR THE STRESS EVOLUTION

Now, by the addition of the creep deformation in the oxide scale and metal substrate in Eq. (5), the total strain of the system in the creep model is expressed as

$$\varepsilon_{ox}(t) = \varepsilon^e_{ox}(t) + \alpha_{ox}\Delta T + \varepsilon^{cr}_{ox}(t) + \varepsilon_g(t)$$

$$\varepsilon_s(z,t) = \varepsilon_s^e(z,t) + \varepsilon_s^{cr}(z,t) + \alpha_s \Delta T \quad , \qquad (11)$$

where ε^{cr} is the creep strain of the system. In terms of the Norton's law, the creep strain is expressed as

$$\dot{\varepsilon}_{ox}^{cr} = J_{ox}\sigma_{ox}^{n}$$

$$\dot{\varepsilon}_s^{cr} = J_s\sigma_s^{m} \quad , \qquad (12)$$

where J is the creep coefficient, m and n are the Norton exponents.

Based on Eqs. (6) and (11) and the generalized Hooke's law, the stress of the system becomes

$$\sigma_{ox}(t) = M_{ox}\varepsilon_{ox}^{e} = M_{ox}\left[\varepsilon_0(t) - k(t)\frac{h_s}{2} - \alpha_{ox}\Delta T - \varepsilon_{ox}^{cr}(t) - \varepsilon_g(t)\right]$$

$$\sigma_s(z,t) = M_s\varepsilon_s^{e} = M_s\left[\varepsilon_0(t) - k(t)z - \alpha_s\Delta T - \varepsilon_s^{cr}(t)\right] \quad . \qquad (13)$$

Differentiating Eq. (13) with respect to time, we have

$$\dot{\sigma}_{ox}(t) = M_{ox}\left[\dot{\varepsilon}_0(t) - \dot{k}(t)\frac{h_s}{2} - \dot{\varepsilon}_{ox}^{cr}(t) - \dot{\varepsilon}_g(t)\right]$$

$$\dot{\sigma}_s(z,t) = M_s\left[\dot{\varepsilon}_0(t) - \dot{k}(t)z - \dot{\varepsilon}_s^{cr}(t)\right] \quad . \qquad (14)$$

For the external oxidation, the substrate thickness is independent of time, differentiation of Eq. (8) gives

$$\int_{-h_s/2}^{h_s/2}\dot{\sigma}_s dz + \dot{\sigma}_{ox}h_{ox} + \sigma_{ox}\dot{h}_{ox} = \sigma_{external}\dot{h}_{ox}$$

$$\int_{-h_s/2}^{h_s/2}\dot{\sigma}_s z dz + \frac{1}{2}\dot{\sigma}_{ox}h_{ox}(h_s + h_{ox}) + \sigma_{ox}\dot{h}_{ox}\left(\frac{h_s}{2} + h_{ox}\right) = \sigma_{external}\dot{h}_{ox}\left(\frac{h_s}{2} + h_{ox}\right) \quad . \qquad (15)$$

Combining Eq. (4) with (12), and then substituting Eq. (14) into (15), we have

$$\dot{k}(t) = -\frac{6(h_s + h_{ox})A_1}{h_s^2}\left[J_{ox}\sigma_{ox}^{n} - \frac{1}{h_s}\int_{-h_s/2}^{h_s/2}J_s\sigma_s^{m}dz + \dot{\varepsilon}_g(t)\right] + A_6(\sigma_{ox} - \sigma_{external})\dot{h}_{ox} + A_7\int_{-h_s/2}^{h_s/2}J_s\sigma_s^{m}z dz \quad , \qquad (16)$$

where

$$A_5 = \frac{3M_{ox}h_{ox}^2 - M_s h_s^2}{M_s h_s^2 + 4M_{ox}h_{ox}h_s + 3M_{ox}h_{ox}^2}$$

$$A_6 = \frac{6\left(h_s^2 M_s + 2M_s h_{ox}h_s + M_{ox}h_{ox}^2\right)}{M_s h_s^2\left(h_s^2 M_s + 4M_{ox}h_{ox}h_s + 3M_{ox}h_{ox}^2\right)}$$

$$A_7 = \frac{-12(M_{ox}h_{ox} + M_s h_s)}{h_s^2\left(h_s^2 M_s + 4M_{ox}h_{ox}h_s + 3M_{ox}h_{ox}^2\right)} \quad . \qquad (17)$$

The stresses in the oxide and the substrate can be calculated by adopting the Euler method, that is

$$\sigma_{ox}(t + \Delta t) = \sigma_{ox}(t) + \dot{\sigma}_{ox}(t + \Delta t)\cdot\Delta t \qquad (18a)$$

$$\sigma_s(z, t + \Delta t) = \sigma_s(z,t) + \dot{\sigma}_s(z, t + \Delta t)\cdot\Delta t \quad . \qquad (18b)$$

The curvature of the system satisfies

$$k(t + \Delta t) = k(t) + \dot{k}(t + \Delta t)\cdot\Delta t \quad . \qquad (19)$$

Substitution of Eqs. (14) and (16) into (18) gives

$$\sigma_{ox}|_{t+\Delta t} = \sigma_{ox}|_t + M_{ox}\left(\dot{\varepsilon}_0|_{t+\Delta t} - \dot{k}|_{t+\Delta t}\frac{h_s}{2} - \dot{\varepsilon}_{ox}^{cr}|_{t+\Delta t} - \dot{\varepsilon}_g|_{t+\Delta t}\right)\cdot\Delta t$$

$$\sigma_s|_{t+\Delta t} = \sigma_s|_t + M_s\left(\dot{\varepsilon}_0|_{t+\Delta t} - \dot{k}|_{t+\Delta t}z - \dot{\varepsilon}_s^{cr}|_{t+\Delta t}\right)\cdot\Delta t \quad . \qquad (20)$$

Equations (16) and (20) are made up of the stress evolution and curvature variation equations.

For simplification, we suppose that the Norton exponents of the system are equal to 1, i.e., $m = n = 1$, which is also done by Panicaud et al.,[24] and Dong et al.[33] Then Eq. (14) becomes

$$\dot{\varepsilon}_0(t) = A_1\left[J_{ox}\sigma_{ox}^{n} + \dot{\varepsilon}_g(t)\right] + \frac{A_2}{h_s}\int_{-h_s/2}^{h_s/2}J_s\sigma_s^{m}dz - \frac{6A_1}{h_s^2}\int_{-h_s/2}^{h_s/2}J_s\sigma_s^{m}z dz + \frac{A_5}{M_s h_s}(\sigma_{ox} - \sigma_{external})\dot{h}_{ox}$$

$$\dot{\sigma}_{ox}(t) = M_{ox}\left[\dot{\varepsilon}_0(t) - \dot{k}(t)\frac{h_s}{2} - J_{ox}\sigma_{ox} - \dot{\varepsilon}_g(t)\right]$$

$$\dot{\sigma}_s(z,t) = M_s\left[\dot{\varepsilon}_0(t) - \dot{k}(t)z - J_s\sigma_s\right] \quad . \qquad (21)$$

Combining Eq. (21) with (15), one obtains

$$M_s\left[\dot{\varepsilon}_0(t)h_s - \int_{-h_s/2}^{h_s/2} J_s\sigma_s dz\right] + \dot{\sigma}_{ox}h_{ox} + \sigma_{ox}\dot{h}_{ox} = \sigma_{external}\dot{h}_{ox}$$

$$M_s\left[-\frac{1}{12}\dot{k}(t)h_s^3 - \int_{-h_s/2}^{h_s/2} J_s\sigma_s z dz\right] + \frac{1}{2}\dot{\sigma}_{ox}h_{ox}(h_s + h_{ox}) + \sigma_{ox}\left(\frac{h_s}{2} + h_{ox}\right)\dot{h}_{ox} = \sigma_{external}\left(\frac{h_s}{2} + h_{ox}\right)\dot{h}_{ox} \quad . \qquad (22)$$

The balance Eq. (8) can be converted as

$$-\int_{-h_s/2}^{h_s/2} J_s\sigma_s dz = J_s\sigma_{ox}h_{ox} - J_s\sigma_{external}\frac{1}{2}(h_{ox} + h_s)$$

$$-\int_{-h_s/2}^{h_s/2} J_s\sigma_s z dz = \frac{1}{2}J_s\sigma_{ox}h_{ox}(h_s + h_{ox}) - \frac{1}{2}J_s\sigma_{external}h_{ox}(h_s + h_{ox}) \quad .$$

By combining the above equations with Eq. (22), we obtain

$$M_s\dot{\varepsilon}_0(t)h_s + M_sJ_s\sigma_{ox}h_{ox} - M_sJ_s\sigma_{external}\frac{1}{2}(h_{ox} + h_s) + \dot{\sigma}_{ox}h_{ox} + \sigma_{ox}\dot{h}_{ox} = \sigma_{external}\dot{h}_{ox}$$

$$-\frac{1}{6}M_s\dot{k}(t)h_s^3 + M_sJ_s(\sigma_{ox} - \sigma_{external})h_{ox}(h_s + h_{ox}) + \dot{\sigma}_{ox}h_{ox}(h_s + h_{ox}) + (\sigma_{ox} - \sigma_{external})(h_s + 2h_{ox})\dot{h}_{ox} = 0 \quad . \qquad (23)$$

Equation (23) can be rewritten as

$$\dot{\varepsilon}_0(t) = -J_s(\sigma_{ox} - \sigma_{external})\frac{h_{ox}}{h_s} + J_s\sigma_{external} - \dot{\sigma}_{ox}\frac{h_{ox}}{M_sh_s} - (\sigma_{ox} - \sigma_{external})\frac{\dot{h}_{ox}}{M_sh_s}$$

$$\dot{k}(t) = J_s(\sigma_{ox} - \sigma_{external})\frac{6h_{ox}(h_s + h_{ox})}{h_s^3} + \dot{\sigma}_{ox}\frac{6h_{ox}(h_s + h_{ox})}{M_sh_s^3} + (\sigma_{ox} - \sigma_{external})\frac{6(h_s + 2h_{ox})\dot{h}_{ox}}{M_sh_s^3} \quad . \qquad (24)$$

Combining Eq. (24) with (14), the stress evolution equations for the oxide scale and the metal substrate are obtained as follows:

$$\left(\frac{M_sh_s^2}{M_{ox}} + 4h_sh_{ox} + 3h_{ox}^2\right)\dot{\sigma}_{ox} + \left[2(2h_s + 3h_{ox})\dot{h}_{ox} + M_sJ_sh_{ox}(4h_s + 3h_{ox})\right](\sigma_{ox} - \sigma_{external}) + J_{ox}M_sh_s^2\sigma_{ox} = -M_sD_{ox}h_s^2\dot{h}_{ox}\dot{\sigma}_s + M_sJ_s\sigma_s$$
$$= -M_s\left[J_s(\sigma_{ox} - \sigma_{external})\frac{h_{ox}}{h_s} + \dot{\sigma}_{ox}\frac{h_{ox}}{M_sh_s} + (\sigma_{ox} - \sigma_{external})\frac{\dot{h}_{ox}}{M_sh_s} - J_s\sigma_{external}\right]$$
$$- M_sz\left[J_s(\sigma_{ox} - \sigma_{external})\frac{6h_{ox}(h_s + h_{ox})}{h_s^3} + \dot{\sigma}_{ox}\frac{6h_{ox}(h_s + h_{ox})}{M_sh_s^3} + (\sigma_{ox} - \sigma_{external})\frac{6(h_s + 2h_{ox})\dot{h}_{ox}}{M_sh_s^3}\right] \quad . \qquad (25)$$

IV. RESULTS AND DISCUSSIONS

To verify the proposed models, FeCrAlY oxidation is discussed at 1000 °C and the parameters for the calculation are listed in Table I.

Figure 2 depicts the relationship of the oxide thickness and time with the stress effect (solid line) and without the stress effect (dash line). It is obviously seen that the oxidation rate with the stress effect becomes smaller than that without the stress effect, which is because the compressive stress in the scale decreases the diffusion

rate according to Eq. (2), and then reduces the chemical reaction. Slower chemical reaction results in slower growth of the scale thickness. This result can also be observed in the experiment.[37]

To compare the proposed model with experimental data[34] and the elastic model,[33] we request the external loading $\sigma_{external}$ to be zero. The stress evolution in the oxide is plotted in Fig. 3. It is seen from Fig. 3 that the stress in oxide of the present model has similar trend to the experiment results of Saunders et al.[34] That is, the stress decreases gradually with the increasing of oxidation time when the oxidation time is larger. However, the stress in oxide dramatically deviates from the experimental results[34] in magnitude and increases with the oxidation time in the elastic model.[33] Moreover, the order of the stress in elastic model reaches ~GPa. On the other hand, the present model exhibits the sharp increase of the oxide stress and there is no experimental data to publish for FeCrAlY oxidation at the initial stage of oxidation, which shows that the present model gives a better approximate stress evolution trend in the oxide scale.

The effect of external loading on the curvature of the system is shown in Fig. 4. The curvature gradually increases as the oxidation time elapses. When the external loading changes from compressive to tensile, the curvature of the system becomes larger and larger which indicates that it is easier to bend for the tensile external loading.

Figure 5 shows the effect of external loading on the variations of oxide scale thickness (the growth rate). With the increasing oxidation time, the thickness of the oxide film gradually increases and the growth rate decreases, constant whatever the external loading is. It can be seen that the compressive external loading reduces the scale thickness significantly as given in Ref. 38 while the tensile external loading increases it as shown in Ref. 39

TABLE I. Value of some material parameters as in Refs. 10, 33, and 34.

Parameter	Symbol (units)	Values
Substrate thickness	h_s (mm)	0.22
Young's modulus of metal	E_s (GPa)	178
Poisson ratio of metal	ν_s	0.33
Young's modulus of oxide	E_{ox} (GPa)	379
Poisson ratio of oxide	ν_{ox}	0.25
Creep coefficient of metal	J_s (Pa^{-1}/s)	2×10^{-14}
Creep coefficient of oxide	J_{ox} (Pa^{-1}/s)	3.0×10^{-15}
Absolute temperature	T (°C)	1000
Activation volume	$\Delta\Omega$ (m^3)	5.164×10^{-29}
Oxidation kinetics constant	k_p ($m/s^{0.5}$)	5.24×10^{-8}
Growth constant	D_{ox} (m^{-1})	42,500
Boltzmann's constant	R	1.38×10^{-38}
Pilling–Bedworth ratio	PBR	1.7857

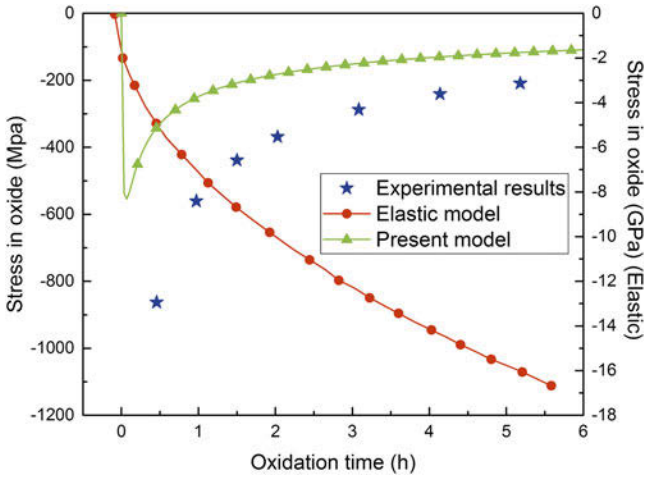

FIG. 3. The comparison of the stress in oxide.

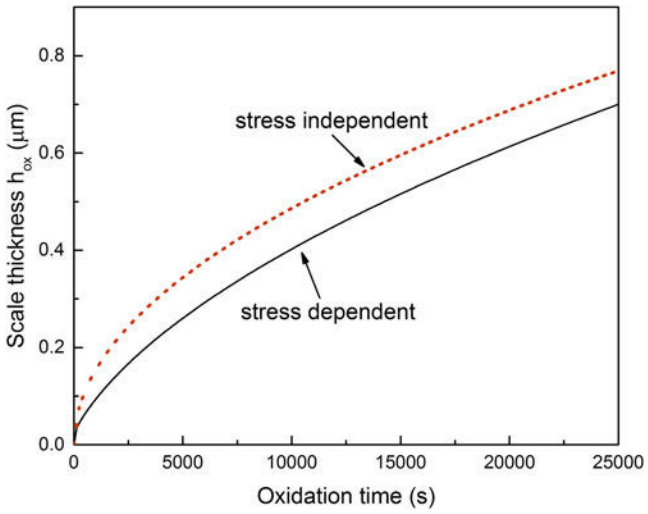

FIG. 2. The comparison of the oxidation kinetics.

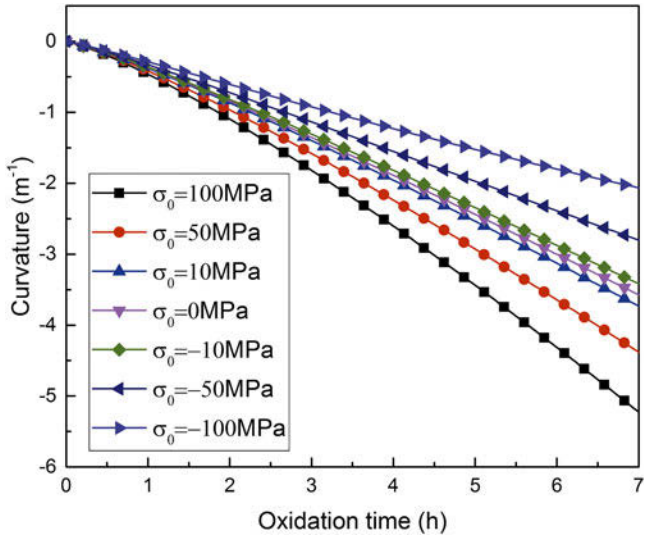

FIG. 4. Effect of external loading on the curvature of system.

and 40. Moreover, the larger the thickness rate is, the larger tensile external loading is, and the smaller the thickness rate is, the larger compressive external loading in magnitude is. Compared with the scale thickness at the same time, it is observed that the thickness of the film becomes smaller and smaller when the external loading changes from the tensile stress to compressive stress which has also been verified in experiments.[37,41]

The variation of the oxide stress in magnitude is also obviously affected by the external loading, as seen in Fig. 6. The stress in the scale is always compressive no matter whether the external loading is tensile or compressive. The oxide stress exhibits a rapid increase at the beginning of the oxidation stage no matter what the external loading is. After the peak, the stress will decrease in magnitude. However, the oxide stress will increase in magnitude when the external loading varies from 100 to −100 MPa. That is, the compressive external loading increases the oxide stress in magnitude while the tensile one decreases it at longer oxidation time. These show that the external loading can control the magnitude of the stress in the oxidation film. Therefore, one may put the tensile external loading to the metal substrate to reduce the oxidation stress.

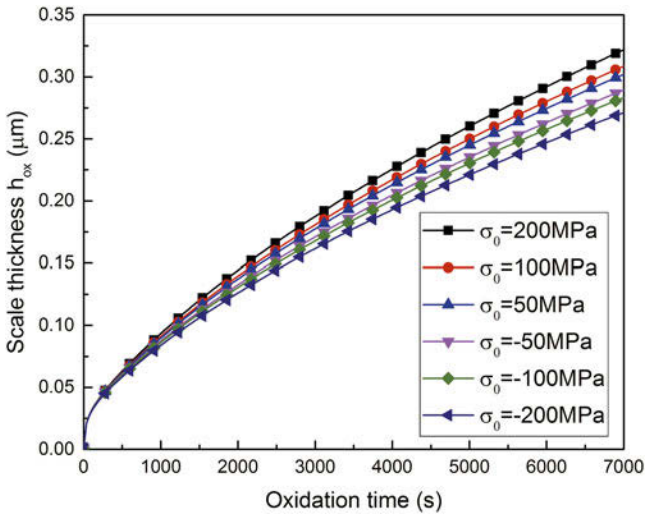

FIG. 5. Effect of external loading on the scale thickness.

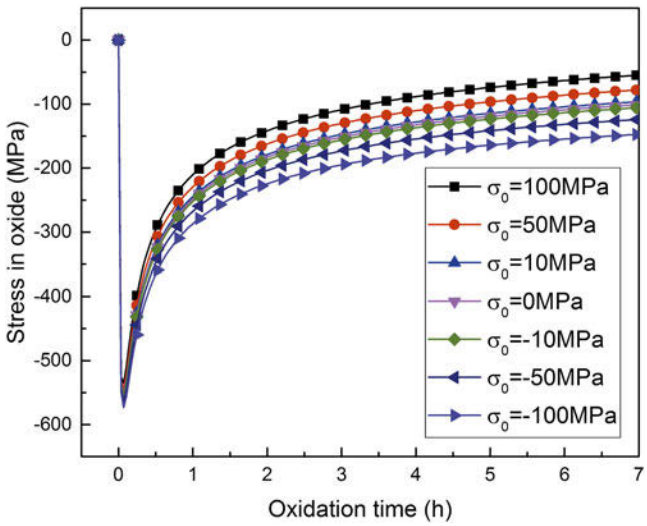

FIG. 6. Effect of external loading on the oxide stress.

V. CONCLUSIONS

Based on the balance equations of forces and moments, a stress evolution model during the metallic oxidation at high temperature is developed by considering the external loading, bending deformation, stress-dependent kinetic relationship. This model exhibits the curvature changes caused by the bending deformation. For FeCrAlY oxidation, the comparison of the oxidation kinetics between stress-dependent and the stress-independent (the parabolic law) is made and results show that the stress reduces the oxidation kinetics. Then the influences of the external loading upon the stress distribution in the oxide scale, the scale thickness and the curvature of the system are investigated, and numerical results show that the tensile external loading decreases the oxidation stress in magnitude while it promotes the growth rate of oxidation layer.

ACKNOWLEDGMENTS

The supports from NSFC (Grants No. 11402054, 11201277), Natural Science Basic Research Plan in Shaanxi Province of China (No. 2015JM1011, 2016JQ1032), Scientific Research Program Funded by Shaanxi Provincial Education Commission (No. 16Jk1504) and Project Funded by China Postdoctoral Science Foundation (No. 2015M570552) are appreciated.

REFERENCES

1. L.C. Stephen: Mechanochemistry: A tour of force. *Nature* **487**, 176–177 (2012).
2. A. Saillard, M. Cherkaoui, and H. EI Kadiri: Stress-induced roughness development during oxide scale growth on a metallic alloy for SOFC interconnects. *Modell. Simul. Mater. Sci. Eng.* **19**, 015009 (2011).
3. D.R. Clarke: The lateral growth strain accompanying the formation of a thermally grown oxide. *Acta Mater.* **51**(4), 1393–1407 (2003).
4. H.E. Evans: Stress effects in high temperature oxidation of metals. *Int. Mater. Rev.* **40**, 1–40 (1995).
5. A. Reddy, D.B. Hovis, A.H. Heuer, A.P. Paulikas, and B.W. Veal: In situ study of oxidation-induced growth strains in a model NiCrAlY bond-coat alloy. *Oxid. Met.* **67**(3–4), 153–177 (2007).
6. L. Hu, D.B. Hovis, and A.H. Heuer: Transient oxidation of a γ–Ni–28Cr–11Al alloy. *Oxid. Met.* **73**(1–2), 275–288 (2010).
7. L.B. Freund and W.D. Nix: A critical thickness condition for a strained compliant substrate/epitaxial film system. *Appl. Phys. Lett.* **69**, 173–175 (1996).
8. T.Y. Zhang, S. Lee, L.J. Guido, and C.H. Hsueh: Criteria for formation of interface dislocations in a finite thickness epilayer deposited on a substrate. *J. Appl. Phys.* **85**(10), 7579–7586 (1999).

9. B. Panicaud, J.L. Grosseau-Poussard, and J.F. Dinhut: General approach on the growth strain versus viscoplastic relaxation during oxidation of metals. *Comput. Mater. Sci.* **42**(2), 286–294 (2008).
10. S. Maharjan, X.C. Zhang, and Z.D. Wang: Effect of oxide growth strain in residual stresses for the deflection test of single surface oxidation of alloys. *Oxid. Met.* **77**(1–2), 93–106 (2012).
11. D.R. Clarke: The lateral growth strain accompanying the formation of a thermally grown oxide. *Acta Mater.* **51**(4), 1393–1407 (2003).
12. A.G. Evans and J.W. Hutchinson: The thermomechanical integrity of thin films and multilayers. *Acta Metall. Mater.* **43**(7), 2507–2530 (1995).
13. C.H. Hsueh and A.G. Evans: Residual stresses and cracking in metal/ceramic systems for microelectronics packaging. *J. Am. Ceram. Soc.* **68**(3), 120–127 (1985).
14. S.M. Hu: Stress-related problems in silicon technology. *J. Appl. Phys.* **70**(6), R53–R80 (1991).
15. C.A. Volkert: Density changes and viscous flow during structural relaxation of amorphous silicon. *J. Appl. Phys.* **74**(12), 7107–7113 (1993).
16. J.L. Grosseau-Poussard, B. Panicaud, and S. Ben Afia: Modelling of stresses evolution in growing thermal oxides on metals. A methodology to identify the corresponding mechanical parameters. *Comp. Mater. Sci.* **71**(7), 47–55 (2013).
17. S.J. Bull: Modeling of residual stress in oxide scales. *Oxid. Met.* **49**(1–2), 1–17 (1998).
18. D.Y. Wang, X.D. Wu, Z.X. Wang, and L.Q. Chen: Cracking causing cyclic instability of $LiFePO_4$ cathode material. *J. Power Sources* **140**(1), 125–128 (2005).
19. A.M. Limarga and D.S. Wilkinson: Modeling the interaction between creep deformation and scale growth process. *Acta Mater.* **55**(1), 189–201 (2007).
20. A.M. Limarga and D.S. Wilkinson: Creep-driven nitride scale growth in γ-TiAl. *Acta Mater.* **55**(1), 25–260 (2007).
21. H.G. Zhou, J.M. Qu, and M. Cherkaoui: Stress-oxidation interaction in selective oxidation of Cr–Fe alloys. *Mech. Mater.* **42**(1), 63–71 (2010).
22. H.L. Wang, Y.H. Suo, and S.P. Shen: Reaction-diffusion-stress coupling effect in inelastic oxide scale during oxidation. *Oxid. Met.* **83**, 507–519 (2015).
23. Y.H. Suo and S.P. Shen: Coupling diffusion-reaction-mechanics model for oxidation. *Acta Mech.* **226**(10), 3375–3386 (2015).
24. B. Panicaud, J.L. Grosseau-Poussard, and J.F. Dinhut: General approach on the growth strain versus viscoplastic relaxation during oxidation of metals. *Comput. Mater. Sci.* **42**(2), 286–294 (2006).
25. S. Maharjan, X.C. Zhang, F.Z. Xuan, Z.D. Wang, and S.T. Tu: Residual stresses within oxide layers due to lateral growth strain and creep strain: Analytical modeling. *J. Appl. Phys.* **110**, 063511 (8 pages) (2011).
26. J.L. Ruan, Y.M. Pei, and D.N. Fang: Residual stress analysis in the oxide scale/metal substrate system due to oxidation growth strain and creep deformation. *Acta Mech.* **223**, 2597–2607 (2012).
27. J.L. Ruan, Y.M. Pei, and D.N. Fang: On the elastic and creep stress analysis modeling in the oxide scale/metal substrate system due to oxidation growth strain. *Corros. Sci.* **66**, 315–323 (2013).
28. S.L. Hu and S.P. Shen: Non-equilibrium thermodynamics and variational principles for fully coupled thermal–mechanical–chemical processes. *Acta Mech.* **224**, 2895–2910 (2013).
29. Y.H. Suo and S.P. Shen: General approach on chemistry and stress coupling effects during oxidation. *J. Appl. Phys.* **114**, 164905(6 pages) (2013).
30. Y.H. Suo and S.P. Shen: Residual stress analysis due to chemo-mechanical coupled effect, intrinsic strain and creep deformation during oxidation. *Oxid. Met.* **84**(3–4), 413–427 (2015).
31. Y. Zhang, X.C. Zhang, S.T. Tu, and F.Z. Xuan: Analytical modeling on stress assisted oxidation and its effect on creep response of metals. *Oxid. Met.* **82**, 311–330 (2014).
32. X.L. Dong, X.F. Fang, X. Feng, and K.C. Hwang: Diffusion and stress coupling effect during oxidation at high temperature. *J. Am. Ceram. Soc.* **96**(1), 44–46 (2013).
33. X.L. Dong, X. Feng, and K.C. Hwang: Oxidation stress evolution and relaxation of oxide film/metal substrate system. *J. Appl. Phys.* **112**, 023502(6 page) (2012).
34. S.R.J. Saunders, H.E. Evans, M. Li, D.D. Gohil, and S. Osgerby: Oxidation growth stresses in an alumina-forming ferritic steel measured by creep deflection. *Oxid. Met.* **48**(3–4), 189–200 (1997).
35. H. Haftbaradaran, H.J. Gao, and W.A. Curtin: A surface locking instability for atomic intercalation into a solid electrode. *Appl. Phys. Lett.* **96**, 091909 (2010).
36. X. Xiao, P. Liu, M.W. Verbrugge, H. Haftbaradaran, and H. Gao: Improved cycling stability of silicon thin film electrodes through patterning for high energy density lithium batteries. *J. Power Sources* **196**(3), 1409–1416 (2011).
37. R.S. Hay: Growth stress in SiO_2 during oxidation of SiC fibers. *J. Appl. Phys.* **111**(6), 063527(13 pages) (2012).
38. H.E. Evans, D.J. Norfolk, and T. Swan: Perturbation of parabolic kinetics resulting from the accumulation of stress in protective oxide layers. *J. Electrochem. Soc.* **125**(7), 1180–1185 (1978).
39. V.K. Tolpygo and D.R. Clarke: Wrinkling of α-alumina films grown by thermal oxidation-I. Quantitative studies on single crystals of Fe–Cr–Al alloy. *Acta Mater.* **46**(14), 5153–5166 (1998).
40. G. Calvarin-Amiri, A.M. Huntz, and R. Molins: Effect of an applied stress on the growth kinetics of oxide scales formed on Ni–20Cr alloys. *Mater. High Temp.* **18**, 91–99 (2001).
41. W. Gauthier, F. Pailler, J. Lamon, and R. Pailler: Oxidation of silicon carbide fibers during static fatigue in air at intermediate temperatures. *J. Am. Ceram. Soc.* **92**(9), 2067–2073 (2009).